SECM at Living Cells

DOI: 10.1002/anie.201301098

Visualization of Oxygen Consumption of Single Living Cells by Scanning Electrochemical Microscopy: The Influence of the Faradaic Tip Reaction**

*Michaela Nebel, Stefanie Grützke, Nizam Diab, Albert Schulte, and Wolfgang Schuhmann**

The respiration activity of an individual living cell is an indicator of its metabolic vitality. Closely positioned microelectrodes have been suggested for determination of the respiration activity by monitoring the local oxygen concentration.[1]

Although first attempts for visualization of the oxygen consumption rate of single living cells by means of scanning electrochemical microscopy (SECM) were already described in 1998,[2] evaluation of the respiratory activity of individual cells remains challenging and the complexity is often underestimated. In particular, the dimensions of the cell itself lead to limitations of conventionally used constant-height mode SECM investigations. Apart from convolution of the oxygen reduction current at the SECM tip with topographic effects, constant-height mode experiments require working distances comparable or below the height of the cell body, thus increasing the risk of tip crash. Attempts to overcome these restrictions include among others positioning of the tip to distances outside the feedback range,[2] embedding of the cells into cavities,[3–5] or efforts to subtract topographic contributions after cell death.[6] Moreover, as living cells are irregular in dimension, the tip-to-cell distance varies with the tip position. Therefore, constant-distance mode (cd-mode) SECM techniques are inherently advantageous for this purpose. In particular, coupling SECM with scanning probe techniques, such as atomic force microscopy (AFM)[7] and scanning ion conductance microscopy (SICM)[8] as well as shearforce[9] and impedance-based techniques,[10] led to efficient strategies to control the tip-to-sample separation. Recently, we described a shearforce-based cd method (4D SF/CD-SECM) that is able to work at various tip-to-sample separations. It can hence detect complete diffusion profiles in the surroundings of sources or sinks of redox-active species.[11]

Although SECM distance control systems are available, the detection of the respiration activity of single living cells remains challenging. Owing to the small rate of oxygen consumption by a single cell, only small current variations ontop of a high background current are measured. Even more importantly, a biological cell acts as an immiscible liquid–liquid interface in a SECM experiment.[12] Lipophilic redox mediators are known to undergo transmembrane diffusion processes and can be utilized to investigate intracellular redox activity.[13,14] However, concentration changes in the vicinity of the cellular membrane, for example by the tip reaction, may induce local concentration gradients and cause a diffusional exchange of redox species over the lipid bilayer in a so-called SECM-induced transfer (SECM-IT) mode.[15] The high solubility of oxygen in lipids promotes this transmembrane diffusion and oxygen can easily cross the cell membrane.[14] This diffusion process superimposes the detection of cell respiration. As a result, in most reports addressing detection of cell metabolism based on the detection of variations in the local oxygen concentration, the positioned microelectrode does not act as a passive observer but actively influences the oxygen concentration inside the gap between tip and cell, resulting in imaging artifacts that have not previously been addressed. Even though mentioned occasionally,[14,16,17] this effect was neglected in SECM investigations of respiration activity at living cells.

Herein, we address the influence of the oxygen reduction rate at the SECM tip on imaging the respiration activity at living cells. We provide strategies to avoid limitations resulting from a strong tip reaction using a potential pulse profile at the tip with a time dependent data acquisition in the shearforce-based cd-mode of SECM.

Commonly, the detection of the local oxygen concentration in close proximity to the cell body is performed by means of a variation of the generator-collector mode of SECM with the tip being continuously polarized at oxygen reduction potential. The tip competes with the respiring living cell for the available oxygen inside the gap between SECM tip and cell surface. Crossing the cell body during a SECM line scan should therefore lead to a decrease of the tip current owing to a locally lowered oxygen concentration caused by cell

[*] Dr. M. Nebel, S. Grützke, Prof. Dr. W. Schuhmann
Lehrstuhl für Analytische Chemie, Elektroanalytik & Sensorik and Center for Electrochemical Sciences, CES
Ruhr-Universität Bochum
Universitätsstrasse 150, 44780 Bochum (Germany)
E-mail: wolfgang.schuhmann@rub.de
Prof. Dr. N. Diab
Chemistry Department; Faculty of Arts and Sciences
The Arab American University
P.O. Box 240, Jenin (Palestine)
Prof. Dr. A. Schulte
Biochemistry-Electrochemistry Research Unit
Schools of Chemistry and Biochemistry, Institute of Science
Suranaree University of Technology
Nakhon Ratchasima 30000 (Thailand)

[**] The authors are grateful to Dr. Dominik Hollatz, Sven Zielke, and Dr. Christian H. Wetzel (Lehrstuhl für Zellphysiologie, Ruhr-Universität Bochum) for the supply of the cell samples, and to Dr. Sonnur Isik-Uppenkamp for her contribution during the initial stage of this project. This work was supported by the EU and the state NRW in the framework of the HighTech.NRW program. M.N. thanks the Ruhr-University Research School funded by Germany's Excellence Initiative for further support [DFG GSC98/1].

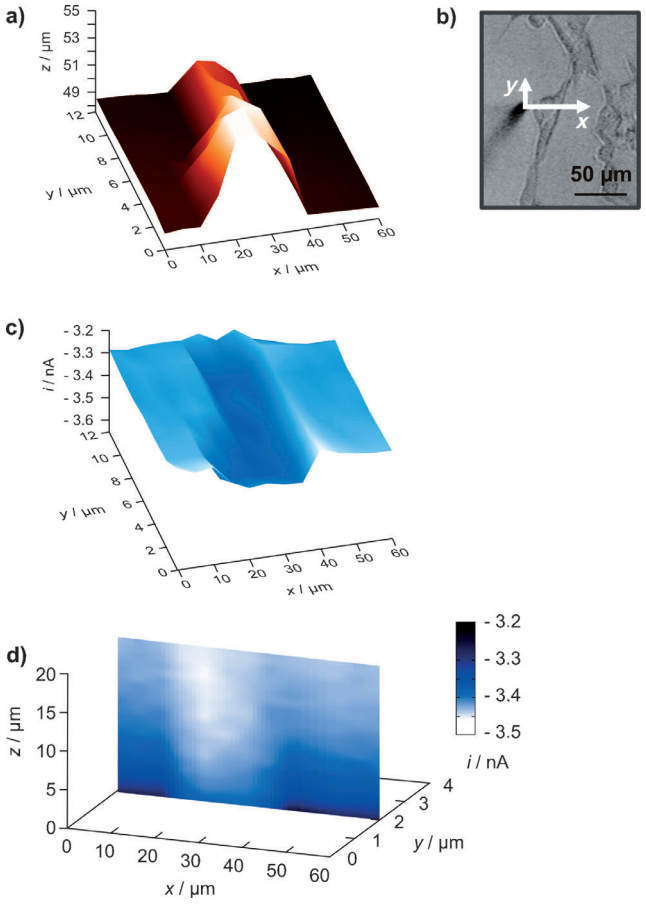

Figure 1. 4D SF/CD-SECM competition experiment at a HEK293 cell with the SECM tip polarized continuously to the oxygen reduction potential. a) Topography image of the obtained from the shearforce-based tip approach at each grid point. b) Photography of the investigated cell and the positioned SECM tip (black dot) taken with the camera of the inverted microscope. c) Current image at the point of shearforce contact ($E_{tip} = -600$ mV). d) Visualization of the oxygen concentration profile above the central cell body (*x*,*z*,*i* image).

respiration. Figure 1 shows a 4D SF/CD-SECM experiment in this competition arrangement at a HEK293 cell. The image of the cell topography is recorded during the shearforce-based approach at each grid point and is displayed as the *z* position of the tip (Figure 1 a). The recorded cell topography is in accordance with the size and shape of the investigated cells as shown in the optical image (Figure 1 b) obtained with the inverted microscope on which the SECM is mounted. Surprisingly, the oxygen reduction current substantially increases when the tip is located above the cell (Figure 1 c). As the tip is retracted at each grid point to predefined constant distance increments above the cell, the distance dependence of the tip current can be visualized by an *x*,*z*,*i* representation (electrochemical tomogram; Figure 1 d).

The observed increase of the tip current reveals the common situation when the driving force of the tip reaction is high enough to locally deplete the oxygen at the outer side of the cell membrane, causing a diffusional compensation of this concentration gradient forcing oxygen to be extracted from the cell. Evidently, the SECM tip is not acting as a passive observer in this case and the results are mainly determined by the tip reaction with a minor influence of cell respiration.

To exclude that the observed current increase is a result of inaccuracies of the tip-to-sample distance control, $[Fe(CN)_6]^{4-}$ was added to the electrolyte during the 4D SF/CD-SECM experiment. As a hydrophilic redox mediator, $[Fe(CN)_6]^{4-}$ does not cross the lipid bilayer and can be used to visualize the cell topography in a negative feedback experiment.[13,14] The simultaneous detection of two different redox species, namely molecular oxygen and $[Fe(CN)_6]^{4-}$, was realized by implementation of a flexible potential pulse profile in the detection scheme of the 4D SF/CD mode (4D SF/CD-RC-SECM), comparable to the implementation of the redox competition mode that has been recently reported for the continuous shearforce-based cd SECM.[18] The topographic linescan (Figure 2, black line) shows the height of the

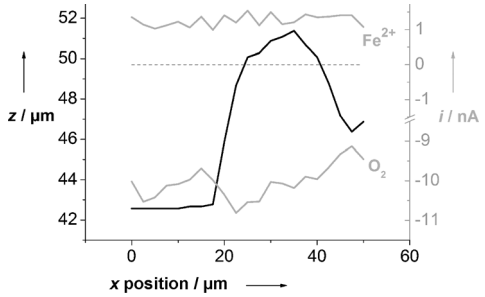

Figure 2. Topographic (black) and current line scan (gray) over a HEK293 cell obtained in constant-distance mode using a potential pulse profile of $E_{tip,base} = 500$ mV, $E_{tip,pulse1} = 500$ mV, $E_{tip,pulse2} = -800$ mV (values taken at $t = 0.5$ s after the application of the potential) in a solution containing 1 mM $[Fe(CN)_6]^{4-}$. The oxygen reduction current increases above the cell body while the $[Fe(CN)_6]^{4-}$ oxidation current remains constant.

cell body to be about 9 µm. While oxygen is drawn from the cell body when the tip consumed oxygen at a high rate resulting in an increased reduction current, no change in the oxidation current of $[Fe(CN)_6]^{4-}$ was detected (gray lines in Figure 2), confirming the accuracy of the distance control.

Basically, three different contributions to the overall tip current can be assumed (Figure 3):

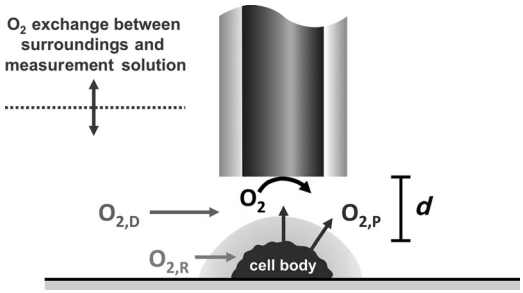

Figure 3. Representation of different oxygen sources contributing to the tip current. $O_{2,D}$: O_2 diffusion from the bulk solution into the gap, $O_{2,R}$: O_2 consumption owing to cell respiration, $O_{2,P}$: O_2 provided by permeation through the cell membrane.

1) The diffusion of oxygen into the gap ($O_{2,D}$) is limited by the tip-to-sample separation d and the size of the SECM tip (RG value). The smaller the working distance, the smaller the contribution of the diffusion of oxygen into the gap to the tip current. However, in the performed constant-distance mode experiment it can be assumed that the contribution is similar at each grid point and for each working distance.

2) Local depletion of oxygen owing to a high reaction rate at the tip leads to a permeation of oxygen ($O_{2,P}$) through the cell membrane. This contribution exclusively depends on the formed concentration gradient between the intracellular medium and the electrolyte solution close to the cell membrane and is therefore independent from the metabolic activity of the investigated cell. The permeation of oxygen should be observed as long as the concentration gradient exists and oxygen is present inside the lipid bilayer or the intracellular medium.

3) The amount of oxygen consumed through respiration of the individual living cell ($O_{2,R}$) is the purpose of the investigation and is assumed to be the smallest contribution to the overall tip current.

The respiration rate f of individual cells from different cell lines have been determined in global experiments to be 10^{-18} mol s^{-1} to 10^{-16} mol s^{-1}.[19] Respiration rates derived from SECM investigations, on the other hand, were on the order of 10^{-16} mol s^{-1} to 10^{-14} mol s^{-1}.[3,5,17,20] The oxygen consumption rate of the SECM tip can be calculated via the diffusion-limited current with $i_{tip} = 4nFDcr$, where D is the diffusion coefficient of oxygen (2.29×10^{-5} cm^2 s^{-1} [21]) and c is the concentration of oxygen (0.25 mM[22]) in water. Assuming a four-electron transfer for the oxygen reduction reaction, the diffusion-limited current i_{tip} is 4.4 nA for a 5 μm radius electrode. With $f_{tip} = i_{tip}/nF$,[17] an oxygen consumption rate of 1.1×10^{-14} mol s^{-1} is obtained for the tip reaction. Oxygen consumption at the polarized SECM tip is several orders of magnitude larger than the consumption of oxygen by an individual living cell.

In principle, three strategies are possible to decrease the extent of the tip reaction: 1) a lower reduction potential at the tip; 2) a smaller electrode size; or 3) short potential pulses or fast-scan cyclic voltammetry[23,24] to avoid an expansion of the diffusion field. Utilization of a potential pulse profile with a time-dependent data acquisition is shown in Figure 4.

The black line represents the topography beginning from the tip positioned above the bottom of the petri dish to the investigated cell. The tip current is displayed at two different times of the competition pulse (gray lines in Figure 4) after the tip is polarized to O_2 reduction potential and competes with the cell for O_2 inside the gap. At short times after application of the oxygen reduction potential, a current decrease is detected above the cells, corresponding to a lower oxygen concentration inside the gap owing to the impact of cell respiration. At increasing times after application of the potential pulse, however, the oxygen reduction current at the tip increases demonstrating the transmembrane diffusion of oxygen. By means of the proposed potential pulse mode, the role of the tip in SECM-based cell respiration imaging can be analyzed and a data acquisition time can be chosen for best imaging contrast (Figure 5).

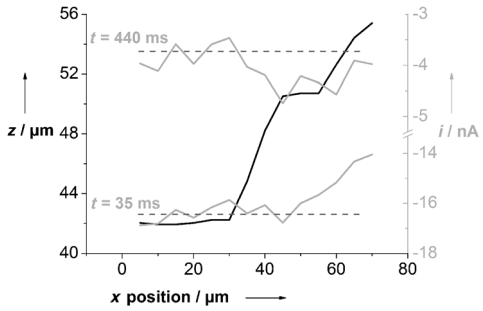

Figure 4. SECM line scans over a HEK293 cell. Topographic line scan (black) and current line scans at different times after applying the oxygen competition pulse at the tip (pulse profile: $E_{tip,base} = 500$ mV, $E_{tip,pulse1} = 500$ mV, $t_{pulse1} = 1$ s, $E_{tip,pulse2} = -350$ mV, $t_{pulse2} = 0.5$ s). It is possible to detect the respiration activity at the beginning of the current detection ($t = 35$ ms), whereas at longer pulse duration ($t = 440$ ms) the transmembrane transport of oxygen occurs.

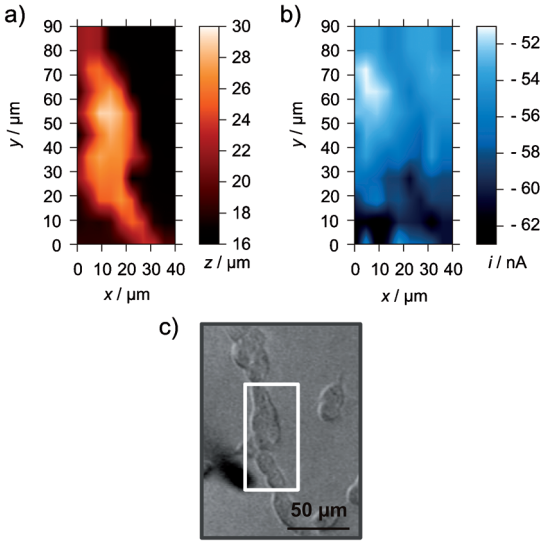

Figure 5. Visualization of the respiration activity of HEK293 cells by 4D SF/CD-RC-SECM. a) Topography image, b) current at the point of closest approach (pulse profile: $E_{tip,base} = 500$ mV, $E_{tip,pulse1} = 500$ mV, $t_{pulse1} = 0.2$ s, $E_{tip,pulse2} = -350$ mV, $t_{pulse2} = 0.5$ s; image taken at $t = 15$ ms), c) optical image of the investigated cell area.

The implementation of a flexible potential pulse profile with a time-dependent data acquisition in the 4D SF/CD mode enabled the characterization of the role of the tip reaction on the oxygen concentration inside the gap between the SECM tip and a living cell. By means of the 4D SF/CD-RC-SECM, a study of cell breathing is even possible without the knowledge of for example the optimal time for data acquisition or the best working distance, and the optimal image can be selected subsequently.

Experimental Section

Human embryonic kidney cells (HEK293) were cultured in Dulbecco's modified eagle medium containing fetal calf serum (10%), non-essential amino acids (1%), and a mixture of penicillin and streptomycin (1%) by standard procedures. The cells were seeded

on plastic petri dishes (Ø 35 mm) at 37 °C in an atmosphere containing 5 % CO_2. Previous to a SECM experiment the culture medium was removed and exchanged by a warmed extracellular solution (140 mM NaCl, 5 mM KCl, 2 mM $CaCl_2$, 1 mM $MgCl_2$, and 10 mM 4-(2-hydroxyethyl)-1-piperazine-1-ethanesulfonic acid (HEPES), pH 7.3).

Polymer-insulated carbon fiber electrodes (Ø 7–9 μm) were used as vibratory disk-shaped tips for all SECM experiments und prepared according to a published procedure.[25,26] A cathodic electrodeposition paint (EDP, ClearClad HSR401 from LVH coatings, UK) was used for the insulation, and the precipitation of the soluble polymer was achieved by applying a constant potential of 6 V for 1 min between the carbon fiber cathode and a ring-shaped Pt counter electrode. Subsequently, heat curing was performed in an oven for 20 min at 180 °C. The deposition of the EDP was repeated for 30 s followed by a second heat-curing step. The active disk face of the carbon fiber electrodes was electroplated with a thin layer of platinum using a solution of 2 mM H_2PtCl_6 (Merck, Darmstadt, Germany) by cyclic voltammetry (300 mV to −500 mV, scanrate: 100 mV s^{-1}, three cycles).

All of the SECM experiments were performed with a specially designed SECM setup for investigation of cell samples (Bio-SECM).[26] Optical shearforce detection was used and the recently described 4D SF/CD-SECM[11] was chosen as the mode of tip movement with a stop criterion of 5–10 % change of the shearforce signal in bulk. A Ag/AgCl (3 M KCl) served as a reference electrode for all of the measurements.

Received: February 6, 2013
Published online: April 29, 2013

Keywords: cell respiration · cells · electrochemistry · oxygen · scanning probe microscopy

[1] a) R. N. Adams, *Anal. Chem.* **1976**, *48*, 1128A; b) R. M. Wightman, D. O. Wipf, *Electroanal. Chem.* **1989**, *15*, 267 – 353; c) S. C. Land, D. M. Porterfield, R. H. Sanger, P. J. S. Smith, *J. Exp. Biol.* **1999**, *202*, 211 – 218.
[2] T. Yasukawa, Y. Kondo, I. Uchida, T. Matsue, *Chem. Lett.* **1998**, 767 – 768.
[3] H. Shiku, T. Shiraishi, H. Ohya, T. Matsue, H. Abe, H. Hoshi, M. Kobayashi, *Anal. Chem.* **2001**, *73*, 3751 – 3758.
[4] a) H. Shiku, T. Shiraishi, S. Aoyagi, Y. Utsumi, M. Matsudaira, H. Abe, H. Hoshi, S. Kasai, H. Ohya, T. Matsue, *Anal. Chim. Acta* **2004**, *522*, 51 – 58; b) Y. S. Torisawa, T. Kaya, Y. Takii, D. Oyamatsu, M. Nishizawa, T. Matsue, *Anal. Chem.* **2003**, *75*, 2154 – 2158.
[5] Y. Torisawa, H. Shiku, T. Yasukawa, M. Nishizawa, T. Matsue, *Sens. Actuators B* **2005**, *108*, 654 – 659.
[6] L. L. Zhu, N. Gao, X. L. Zhang, W. R. Jin, *Talanta* **2008**, *77*, 804 – 808.
[7] J. V. Macpherson, P. R. Unwin, A. C. Hillier, A. J. Bard, *J. Am. Chem. Soc.* **1996**, *118*, 6445 – 6452.
[8] D. J. Comstock, J. W. Elam, M. J. Pellin, M. C. Hersam, *Anal. Chem.* **2010**, *82*, 1270 – 1276.
[9] a) M. Ludwig, C. Kranz, W. Schuhmann, H. E. Gaub, *Rev. Sci. Instrum.* **1995**, *66*, 2857 – 2860; b) B. Ballesteros Katemann, A. Schulte, W. Schuhmann, *Chem. Eur. J.* **2003**, *9*, 2025 – 2033; c) P. I. James, L. F. Garfias-Mesias, P. J. Moyer, W. H. Smyrl, *J. Electrochem. Soc.* **1998**, *145*, L64 – L66.
[10] M. A. Alpuche-Aviles, D. O. Wipf, *Anal. Chem.* **2001**, *73*, 4873 – 4881.
[11] M. Nebel, K. Eckhard, T. Erichsen, A. Schulte, W. Schuhmann, *Anal. Chem.* **2010**, *82*, 7842 – 7848.
[12] S. Amemiya, J. D. Guo, H. Xiong, D. A. Gross, *Anal. Bioanal. Chem.* **2006**, *386*, 458 – 471.
[13] B. Liu, S. Rotenberg, M. Mirkin, *Proc. Natl. Acad. Sci. USA* **2000**, *97*, 9855 – 9860.
[14] B. Liu, W. Cheng, S. A. Rotenberg, M. V. Mirkin, *J. Electroanal. Chem.* **2001**, *500*, 590 – 597.
[15] A. L. Barker, J. V. Macpherson, C. J. Slevin, P. R. Unwin, *J. Phys. Chem. B* **1998**, *102*, 1586 – 1598.
[16] a) Y. Takahashi, A. I. Shevchuk, P. Novak, Y. Murakami, H. Shiku, Y. E. Korchev, T. Matsue, *J. Am. Chem. Soc.* **2010**, *132*, 10118 – 10126; b) K. Nagamine, Y. Takahashi, K. Ino, H. Shiku, T. Matsue, *Electroanalysis* **2011**, *23*, 1168 – 1174.
[17] Y. Takahashi, Y. Hirano, T. Yasukawa, H. Shiku, H. Yamada, T. Matsue, *Langmuir* **2006**, *22*, 10299 – 10306.
[18] A. Schulte, M. Nebel, W. Schuhmann, *Methods Enzymol.* **2012**, *504*, 237 – 254.
[19] P.-A. Ruffieux, U. von Stockar, I. W. Marison, *J. Biotechnol.* **1998**, *63*, 85 – 95.
[20] M. Nishizawa, K. Takoh, T. Matsue, *Langmuir* **2002**, *18*, 3645 – 3649.
[21] D. Pletcher, S. Sotiropoulos, *J. Electroanal. Chem.* **1993**, *356*, 109 – 119.
[22] E. S. Smotkin, F. T. Moy, W. Z. Plachy, *Biochim. Biophys. Acta Biomembr.* **1991**, *1061*, 33 – 38.
[23] D. S. Schrock, J. E. Baur, *Anal. Chem.* **2007**, *79*, 7053 – 7061.
[24] K. L. Adams, M. Puchades, A. G. Ewing, *Annu. Rev. Anal. Chem.* **2008**, *1*, 329 – 355.
[25] A. Schulte, R. H. Chow, *Anal. Chem.* **1996**, *68*, 3054 – 3058.
[26] L. P. Bauermann, W. Schuhmann, A. Schulte, *Phys. Chem. Chem. Phys.* **2004**, *6*, 4003 – 4008.

